Eur Biophys J (1999) 28: 516–525

BIOPHYSICS LETTER

Heiko Zimmermann · Rolf Hagedorn
Ekkehard Richter · Günter Fuhr

Topography of cell traces studied by atomic force microscopy

Received: 11 January 1999 / Revised version: 1 April 1999 / Accepted: 8 April 1999

Abstract Migrating adherent cells release material onto artificial substrates like glass and silicon while moving. Traces of mouse fibroblasts (L929) have been visualised by atomic force microscopy (AFM). "Non-contact" mode AFM in a liquid environment can extract topographic information from these traces. This dynamic mode allows the study of these soft structures without damage or compression. The AFM images show crossing and branching networks (with specific angles of branching), structured patches, nodular elements, linear elements with irregular height and other features. Fourier analysis of segment spacing in the strands is presented. These spatial features of fibroblast traces are strong indications that actin linked to structural proteins is involved in the formation of cell traces. We also give methods for trace preparation and undistorted imaging and discuss further perspectives.

Key words Fibroblast · Non-contact mode · Filaments · Dendritic networks · Branches

Introduction

Since the invention of the atomic force microscope (AFM or scanning force microscope) by Binnig et al. (1986), this method has become a powerful tool in life sciences and biophysics (Erlandsson and Olsson 1994; reviewed by Henderson 1994). Major advantages of this method are (1) the possibility of imaging in liquid environments (studying biological samples in situ or in vitro) (Drake et al. 1989; Butt et al. 1991), (2) a wide range of resolution, spanning nanometers and micrometers (Radmacher et al. 1992), (3) the ability to detect forces in the pN range (Florin et al. 1994), (4) the possibility of measuring elastic properties (Hofmann et al. 1997) and (5) the different modes of operation (Krüger et al. 1997). AFM has been used in biology to image macromolecules (Oberleithner et al. 1997; reviewed by Ikai 1996), cell organelles (Fritz et al. 1994), cell surfaces and membranes (Hoh and Schoenenberger 1994; Bustamante et al. 1995; Hörber et al. 1995). The contact mode has been applied in the study of the cytoskeleton (Hofmann et al. 1997).

Scanning whole cell surfaces under liquid or physiological conditions presents three main problems. Firstly, adherent cells can exhibit a topography too complex for the scanner. Secondly, cell surfaces are highly dynamic, requiring fast scanning rates. Thirdly, cells can contaminate the scanning tip. Recently, however, some success has been achieved using modes with modulated forces (Hansma et al. 1994).

In this work we present a new application of AFM that differs from the examples given above: the imaging of traces released by individual cells on artificial substrates. It is well known from numerous light-microscopy observations that cells like fibroblasts, macrophages and cancer cells release or remove material during adhesion and active migration (Chen 1981; Hay 1985; Bereiter-Hahn and Vöth 1988). The formation and breakage of cell-substrate or cell-cell contacts is a fundamental physiological phenomenon of cell adhesion, migration and cytoskeletal operation (Palecek et al. 1996; Small et al. 1996). However, except for some molecular characterisations (Yamagata et al. 1993; Palecek et al. 1996), cell traces are little investigated. This is probably because the typical dimensions of traces are near or below the resolution of conventional microscopy.

During our studies of growth and cryo-conservation of adherent cells on micro-structured surfaces (Hornung et al. 1996; Richter et al. 1996), we observed that migrating fibroblasts regularly release considerable amounts of material. The structure of these traces depends on the cell type, the surface coating and some

H. Zimmermann · R. Hagedorn · E. Richter · G. Fuhr (✉)
Lehrstuhl für Membranphysiologie, Institut für Biologie,
Mathematisch-Naturwissenschaftliche Fakultät I,
Humboldt-Universität zu Berlin, Invalidenstrasse 42,
D-10115 Berlin, Germany
e-mail: g.fuhr@webserv.biologie.hu-berlin.de

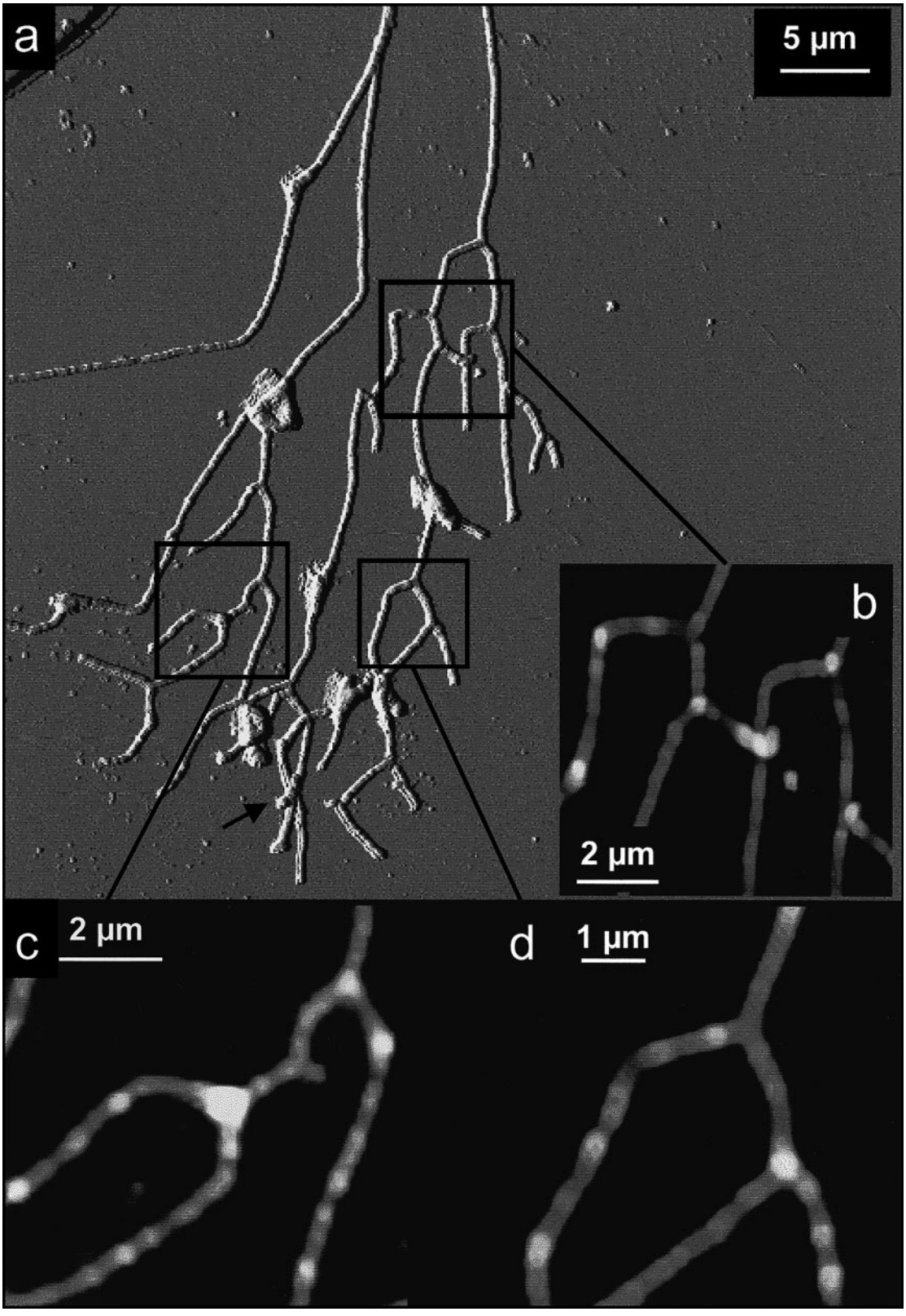

Fig. 1 **a** Non-contact AFM topography image of a cell trace (wet fixed). The trace was produced by one L929 cell (not shown). The direction of movement was from the bottom to the top of the picture. Several branch points give an overall dendritic appearance. The trace also shows an overlapping of several strands (*black arrow*). The feature at the top left is a part of the CELLocate structure (glass substrate). **b** Rescan of three branches of the trace. The branching angles are 95°, 95° and 90° (*from left to right*). **c** Another close-up of the branches. The angles are 90° (*right*) and 95° (*left*). **d** Rescan of a smaller area with higher resolution. This greyscale depiction shows two typical branches: one of increased height (*white point* on branch centre) and one without any increase. The angles are 90° and 100°

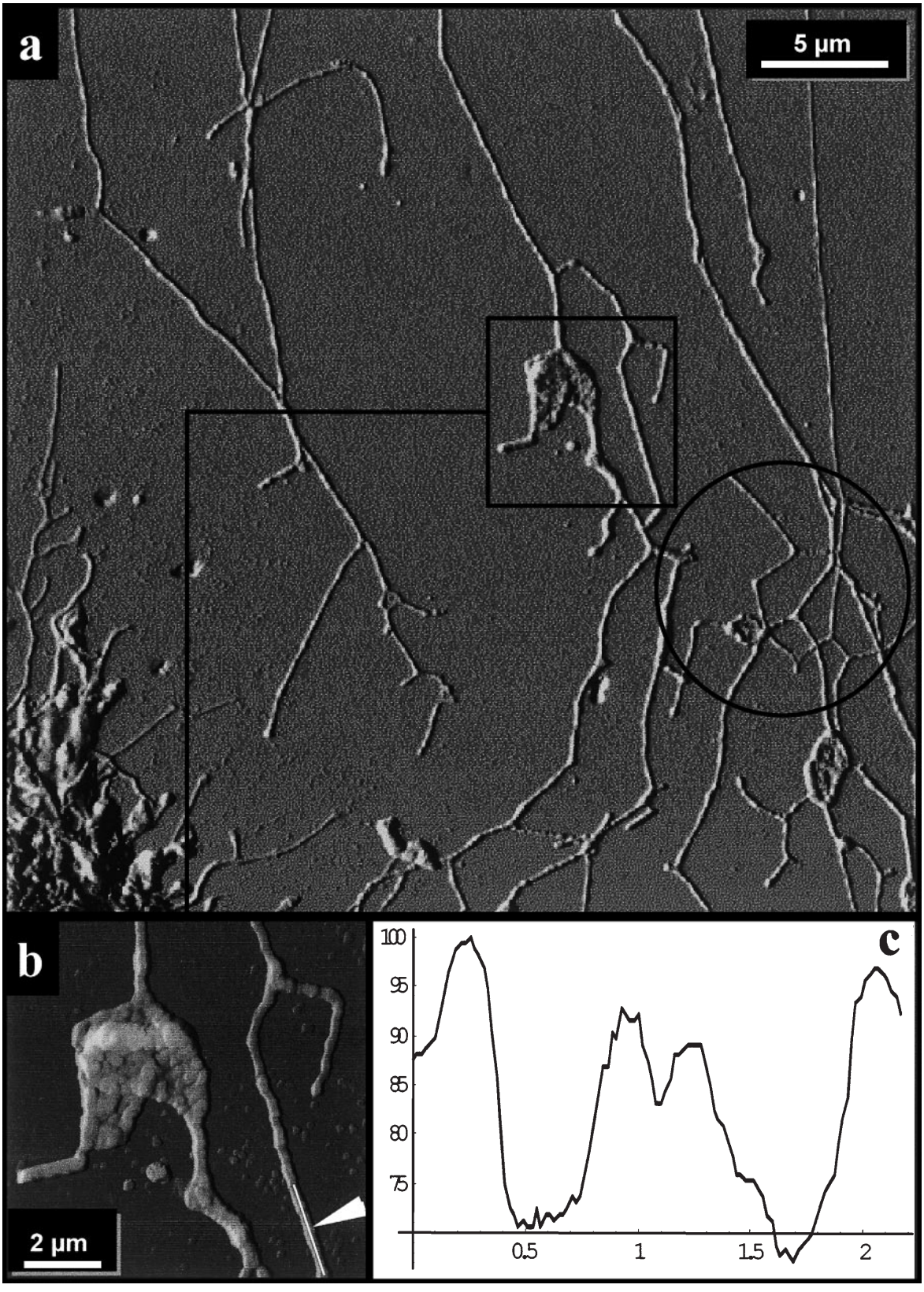

Fig. 2 **a** Non-contact AFM topography image ("shadowed") of several cell traces (wet fixed). Traces were produced by L929 cells. A part of one donor cell can be seen bottom left. The image shows the undistorted overlapping of traces (*circle*). For more details, see text. **b** A close-up of a patch from **a**. The image is shadowed and therefore the surface structure of the patches can be seen. The *white line* on the trace in the lower right corner indicates where the linescan **c** was taken (*white arrow*). **c** Linescan along a trace. Relative height in percent of maximum versus distance in microns is drawn. Height and height modulation can be seen

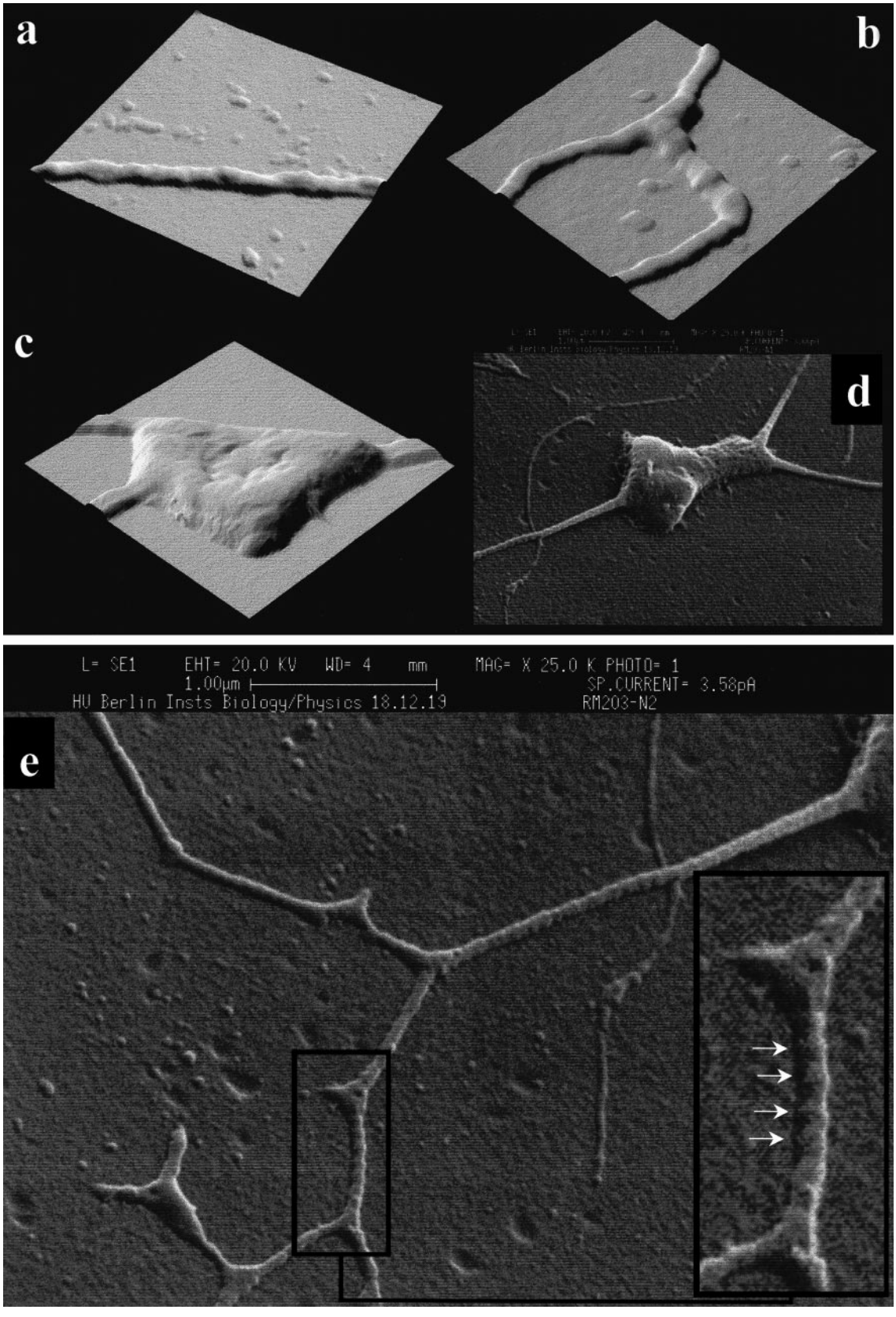

Fig. 3a–e A catalogue of several basic elements imaged with AFM and SEM. AFM images of linear elements (**a**) and (**b**) and a nodular element (**c**). **d** A similar nodular element imaged with SEM. Note that the elements are enveloped with a membrane and can, therefore, be influenced osmotically (unpublished). To compare AFM imaging of cell traces with SEM imaging, another SEM image is depicted in **e**, where even the height modulation can be seen (*white arrows* in the close-up, right). Size of pictures are: **a** 4 µm, **b** 3.5 µm, **c** 4.5 µm, **d, e** 4.9 µm (width)

other parameters. Recently we showed that cell traces are well-organised, membrane-enveloped structures composed of linear and nodular elements as well as patches with typical dimensions in the sub-micron range [width and height: several hundred nanometers, up to several hundred micrometers in length (Fuhr et al. 1998)]. Higher-order structures (dendritic and point patterns) were found and a first microanalysis was presented. Although traces from a single cell can cover several thousands of square micrometers, the total amount of released material is 1% or less of the cell volume. Although the physiological role, if any, is not clear up to now, traces may serve as a "footprint" of individual cells, giving information and insight into cell activity, physiological status and the composition of membrane and cytoplasm.

To visualise cell traces we applied different microscopic techniques such as atomic force microscopy (AFM), interference reflection microscopy (IRM) and scanning electron microscopy (SEM) (Fuhr et al. 1998). In this paper we show that AFM is especially suited to the imaging and characterisation of the topography of cell traces. Additionally, the static traces give information about the dynamics of cell adhesion, processes of migration and some new hints related to the molecular machinery of the cytoskeleton.

Materials and methods

Biological preparations

Mouse fibroblasts, cell line L929, were obtained from Deutsche Sammlung von Mikroorganismen und Zellkulturen (DSM, Braunschweig, Germany). Cells were cultured in RPMI 1640 medium with 5% fetal calf serum (FCS) in a humidified incubator under 5% CO_2 in air. The confluent cells were split twice a week using 0.05/0.02% trypsin/ethylenediaminetetraacetic acid at 37 °C for 3–5 min. To remove the enzyme, the cells were subjected to 2–3 washing cycles with the culture medium. Harvested cells were counted in a THOMA counting chamber and seeded into fresh medium at 1×10^4 cells/ml. Experiments were carried out with cells cultivated for one day in a subculture. Harvested cells were diluted in the culture medium to a final concentration of 1×10^3 cells/ml and seeded into Corning disposable multiple well plates (4 wells, 1 ml/well). At the end of the cultivation period, the samples were washed three times with warmed phosphate-buffered saline (PBS) and fixed with 2.5% glutaraldehyde in PBS for 15–30 min. The AFM imaging of the traces was performed in ultrapure water (Millipore).

AFM techniques

The AFM experiments were carried out with an Explorer AFM (TopoMetrix, Darmstadt, Germany) in the non-contact mode, where the change of the vertical cantilever oscillation amplitude is detected. Standard pyramidal silicon nitride cantilevers (type 1530-00 from TopoMetrix) suitable for scanning in a liquid medium were used. The AFM was combined with a modified inverted optical microscope (Zeiss, Jena, Germany) for localising those cell traces preselected with the confocal laser scanning microscope (Leica Lasertechnik, Heidelberg, Germany) in the reflection mode. Samples were fixed with glutaraldehyde on sterile CELLocate (square size 175 μm, Eppendorf-Netheler-Hinz, Hamburg, Germany) and scanned in ultrapure water. The images were obtained with a TopoMetrix AFM liquid tripod-scanner, model 5180-00 with a nominal 12 μm range perpendicular to the sample. Maximum scan range was 100 μm. Calibration and "crosstalk" (that is, calibration of angle measurements) were done using a Si/SiO_2 grid (TopoMetrix). The feedback parameters (PID settings) for the non-contact mode were optimised by minimising the changes in the amplitude signal (constant force mode). Scanning frequencies were usually in the range of 0.5–1 Hz per line and were increased for smaller samples to minimise time-dependent scanner effects.

Image processing was performed using SPMLab software (TopoMetrix). Images were treated in two ways. (1) To show structure heights, greyscale images were flattened (2D or three-point levelled) and histogram corrected (linear height scale). (2) To show small structures of the cell traces, a pseudo-3D view was calculated using the "shadow" function of the software, which means that a virtual light source is set to the left (differential view). The result of this function is an image where height information is lost, but small corrugations are emphasised – similar to the deflection signal in the contact mode, but based on the *z* piezo signal instead of the deflection signal of the cantilever.

Other techniques

The protocol of the preparation and carrying out of the SEM measurements can be found in Fuhr et al. (1998).

►

Fig. 4a–f Typical part of a segmented cell trace produced by L929 fibroblast (AFM image). **a** "Shadowed" depiction of two strands of the trace. A branch can be seen (*bottom right*). **b** Greyscale image of a close-up in the linear part of the left strand of **a**. **c** Image **b** rotated 10° anticlockwise. **d** One-dimensional Fourier spectrum in *y*-direction (that is, vertical) of **c**. The filled graph (*left*) is linearly scaled; the *right* is the same data on a logarithmic scale; the units of the *x*-axes are reciprocal microns, the *y*-axes are in arbitrary units. The peak at 0.75 μm^{-1} can be seen. **e** Filtered image of **c**. The frequency 0.75 μm^{-1} was taken for the inverse Fourier transformation. The disturbance on the right side is caused by the second trace strand in **c**. **f** A close-up of the lowest trace segment ("shadowed"). The *arrows* indicate the points that appear in the filtered image. For more details, see text

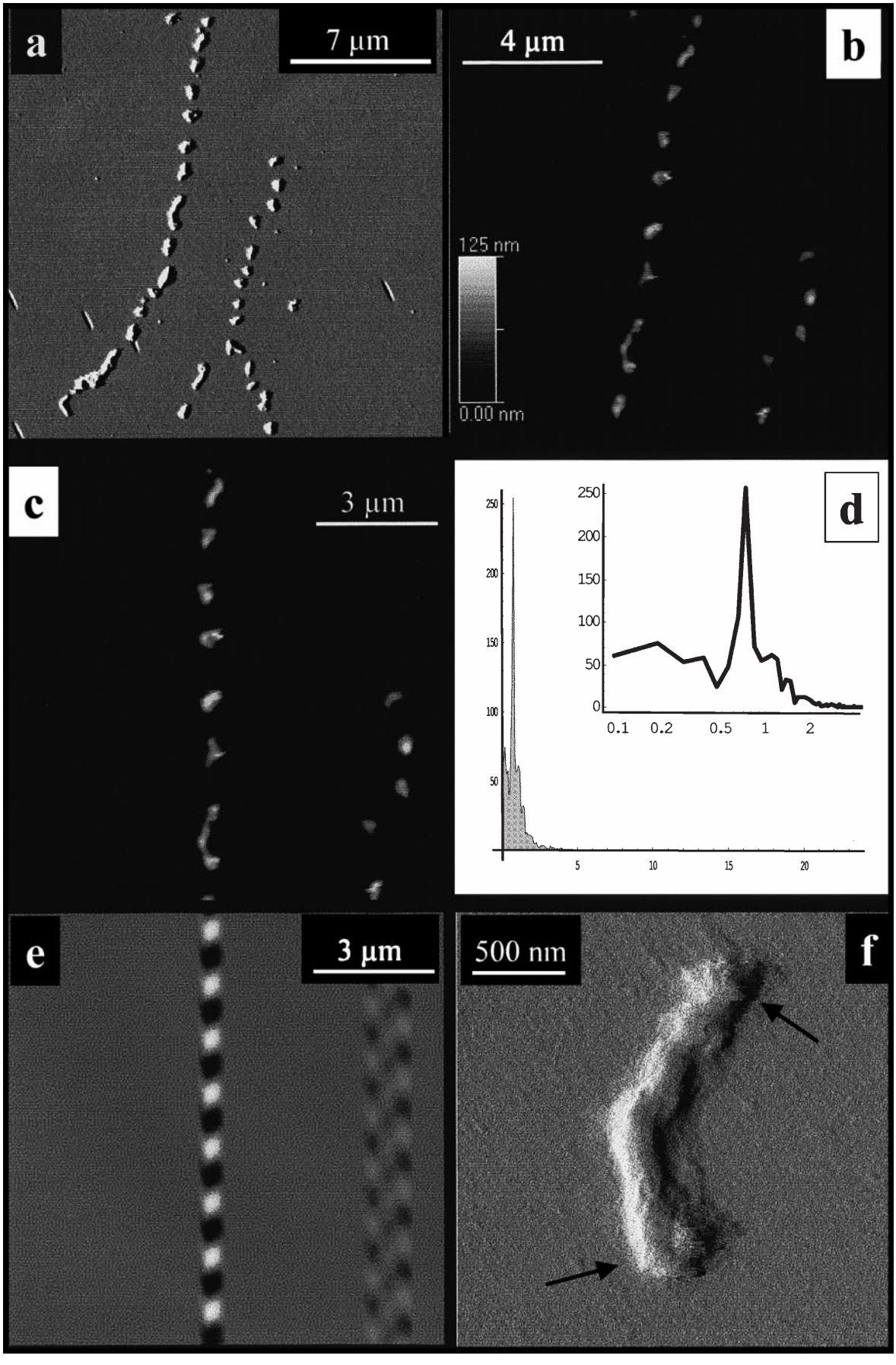
a
7 µm
4 µm
b
125 nm
0.00 nm
c
3 µm
d
250
200
150
100
50
0
0.1
0.2
0.5
1
2
5
10
15
20
e
3 µm
500 nm
f

Results

Figure 1a is an overview of a dendritic trace of a single cell. Filaments, nodular elements and patches are visible. The dendritic impression is caused by the arrangement of the branches: two strands of the trace unite into one strand in the direction of cell movement. The black arrow indicates a location where two strands of the trace overlap. The image is shadowed (for detail see Materials and methods) and therefore quantitative height information is lost. Figure 1b–d shows close-ups of several branches in the greyscale mode. It can be seen that centres of branches are often significantly higher (white) than the rest of the surface, which is itself of varying height. This modulation seems sometimes nearly periodic over small intervals (bottom right in d) and sometimes very inhomogeneous (rest). The value of the branching angles are in the range of 90–100°.

Figure 2a is an overview of the traces of several cells. Traces from different cells can overlap without distortion. The rescan with higher resolution in Fig. 2b shows that patches of the trace can have structures on their surface. Here, the pattern is quite regular. Similar structures on the linear elements of the trace show variations of the trace height. The cross-section (Fig. 2c) shows that the variation can be 30% or more of the maximum height (the y-axis is relative height in percent of maximum height). Typical values for the trace height are in the range of 70–100 nm; patches and other discrete structures can reach heights of more than 200 nm.

In Fig. 3, AFM images of several basic elements are compared with scanning electron images. Although the SEM preparation requires dehydration, the similarity of visualisation between the techniques is clearly demonstrated. Even the modulation of height can be seen (Fig. 3e).

Figure 4 deals with the regularity of segmented traces. The fact that these segmented traces do not contain F-actin is reported in Fuhr et al. (1998). Figure 4a shows the area of interest of a segmented trace. It can be seen that parts of the trace are very homogeneous. In Fig. 4b the linear homogeneous part of Fig. 4a is depicted in greyscale mode. To prove the regularity this image was rotated 10° anticlockwise to align the trace to the y-direction (that is, vertical) and a one-dimensional Fourier analysis in the y-direction was performed. The spectrum is shown in Fig. 4d in linear scale and logarithmic scale. The dominant frequency can be seen: the peak at $k = 0.75\ \mu m^{-1}$. The corresponding period (r-value) is 1.34 μm. The inverse Fourier transform of this frequency is shown in Fig. 4e. The similarity to the original image is obvious. Figure 4f shows a close-up of the lowest item of Fig. 4c in shadow mode. An interesting detail of this image is that the ends of the imaged item (indicated with black arrows) are exactly at the period mentioned above.

In Fig. 5, AFM images of the nearfield of a trace producing cell is shown. Imaging nearfield can give information about the formation of cell traces because the transition between the donor cell and the "normal" traces presented above can be seen. In the close-up (Fig. 5c) the meniscus of the membrane spanning two fibres, that are obviously thicker than traces, can be seen.

Discussion

Cell traces are especially amenable to force microscopy because they are well connected to the substrate and static when far enough from the donor cell. They have suitable dimensions for force microscopy, being high enough to give a good signal-to-noise ratio and small enough to be within the scanner range, which is 10 μm. The lateral extent of the traces means that AFM images can be checked by complementary methods (for example, electron microscopy or confocal laser scanning microscopy; for details see Fuhr et al. 1998), and vice versa. However, atomic force microscopy is the only method that can visualise topographical features without dehydrating the traces.

Nevertheless, careful imaging is necessary to avoid damaging the traces. Our experience with force microscopy of cell traces has shown that dynamic modes of operation – like the non-contact mode – are the methods of choice because of minimising lateral shear stress. The figures show that clear images can be achieved with the non-contact mode. Given the right imaging parameters (that is, lowest force which gives contrast, and low scan speed), the absence of distorting lines in the direction of the scan shows that the traces are not damaged by lateral forces (Braet et al. 1997a). We apply only very small forces for a short time to the trace and this method seems to be effectively non-invasive.

The overlapping of traces from different donor cells is interesting with regard to the question of the formation and function of the traces. This overlapping is a strong hint that cells crossing the pathways of other cells are not influenced by the trace. We have seen traces which influence the subsequent motion of the donor cell. However, we have not yet seen evidence of traces influencing the locomotion of other cells of the same type. As reported in our recent paper (Fuhr et al. 1998), the phenomenon of cell traces in the form of branching networks is not restricted to mouse L929 fibroblasts. Without doubt, trace formation is closely related to the activity of the cytoskeleton near the enveloping membrane, involving actin polymerisation and depolymerisation (Sackmann 1994). There are strong indications, for example the presence of F-actin (Fuhr et al. 1998) in non-segmented traces and the regularity of segmented traces (Fig. 4), that structuring proteins and actin aggregation influence the trace pattern.

The fixed angles of branching, that give the traces their characteristic appearance, indicate a chemical influence. Such clear defined angles and the same dendritic

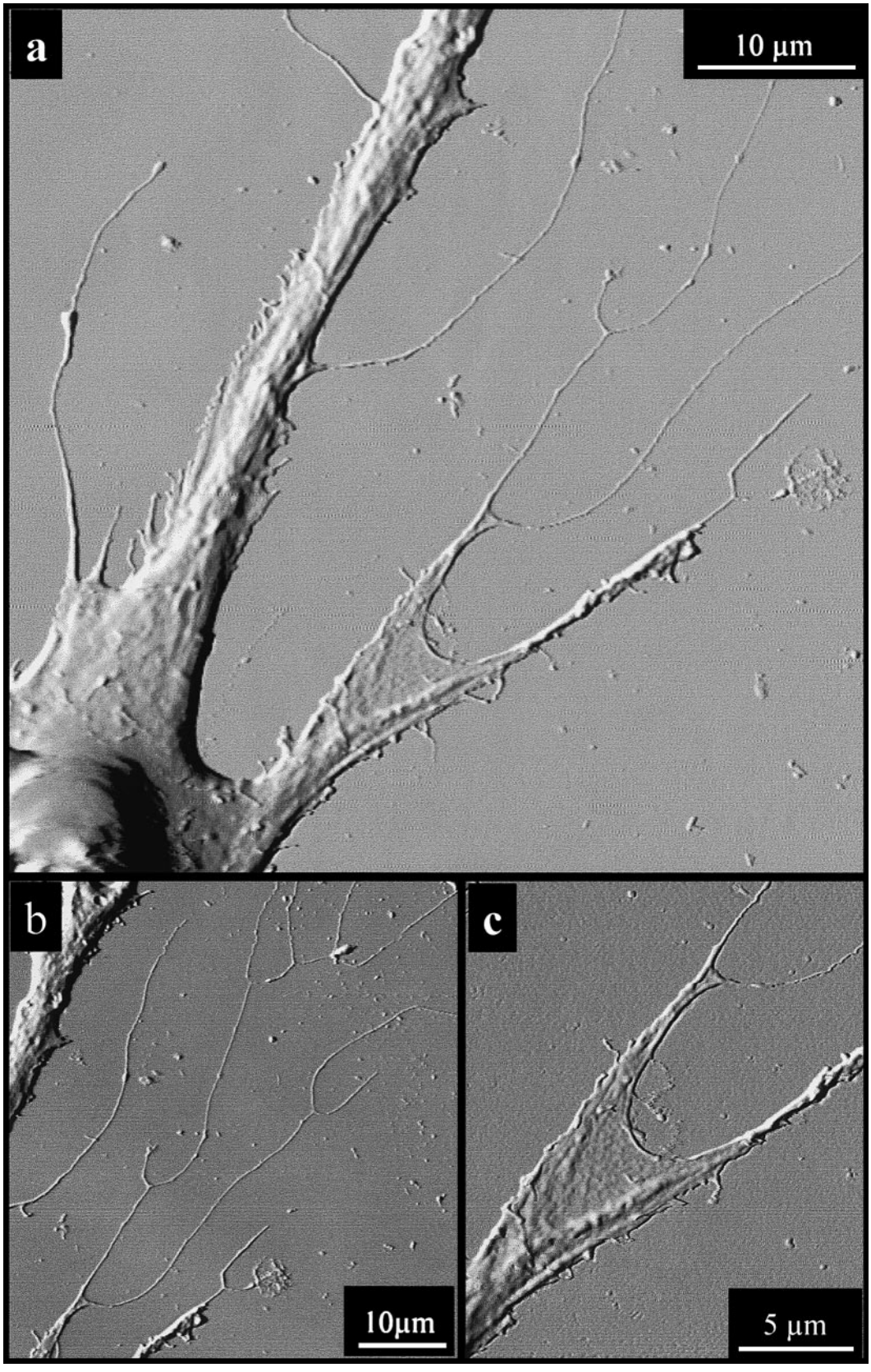

Fig. 5a–c L929 cell traces near the cell body (so-called near field). All images are in the shadow mode. **a** AFM image of a part of a trace-producing cell with a part of the nearfield trace. **b** The image in the region of the traces (overlaps top right of **a**). **c** Close-up of the area of transition between the end of a cell and the beginning of a trace. For more details, see text

shape can be found also at the molecular level, e.g. at the arp2/3-actin linkage (Mullins et al. 1998). The different values of the angles (70° measured on the molecular arp2/3-linked actin and 90° measured on the traces) could be caused by higher-order structures and mechanical stress during trace release. The arp2/3 complex is discussed because actin is implicated in the formation of branched networks (Mullins et al. 1998). Arp2/3 complexes are composed of actin-related proteins and their subunits can be found in all eukaryotes (Welch et al. 1997). Welch et al. (1997) showed that the arp2/3 complex is localised at the border of the fibroblast lamellipodium. This part of the cell is highly dynamic during movement and trace formation. Note that we measure angles over a structure of about 2 μm in size (Fuhr et al. 1998), whereas the measurements of the branching angles on the molecular level of arp2/3 are based on structure sizes of several tens of nanometers (Mullins et al. 1998).

It should be emphasised that factors other than the arp2/3-actin linkage could also influence the measured branching angle. Looking at Fig. 5, the membrane might play an important role. Figure 5c indicates a connection between the meniscus of a membrane spanning two fibres in the cell and the formation of branches (Fig. 5c top).

Force imaging can give three-dimensional structure information. We found height modulation of about 30%. Because of the ability of the AFM to measure in liquid, we can be sure that the modulation is not an artefact of dehydration (a detailed comparison of the shrinking of cell structures with different preparations for scanning electron microscopy and atomic force microscopy can be found in Braet et al. 1997b). The modulation of the cell trace height is not regular. Even though there are short segments with similar changes in height, there is no overall periodic structure. A possible explanation could be the decoration of the filament inside with macromolecules. Irregularities of such decorations have been reported (Mullins et al. 1997). Of course, other explanations like an elastic kick of the outer membrane while breaking from the donor cell could also be true. One aspect of the *z*-structure was the increased height of the branch centres. Here again, an actin-related or actin-binding protein analysis is greatly needed.

Figure 4 shows that Fourier analysis applied to AFM data can prove the regularity of topographical features. Future experiments combining this method with dynamic investigations will show whether the regularity arises from a time periodic process or from a supramolecular structure.

Summarising, AFM is a valuable, nearly non-invasive tool for studying the topography of cell traces. The additional height and topography information complements the knowledge about trace structure. A more detailed classification of the basic elements, for example branches with and without an increased centre, can be achieved with non-contact imaging in a liquid environment. Cell traces are a new application for scanning force microscopy in the field of cell adhesion and locomotion. In addition to their content of molecular information (membrane composition, receptors, cytoplasmic components and, possibly, genetic material) and diagnostic relevance, they might be used as highly organised submicron elements produced by cells and useable for biotechnological or bioelectronic purposes. Further relations to and applications in the field of surface characterisation, e.g. for implants (Zimmermann et al. 1992; Hasse et al. 1997) or artificial tissues, are imaginable.

Acknowledgements We are grateful to S. G. Shirley for helpful discussions, H. Niehus for use his AFM and S. Rogaschewski for carrying out the SEM imaging. Microstructured surfaces were granted by the Bundesministerium für Bildung und Forschung BMBF (grant no. 0310887). This work was supported by the Deutsche Forschungsgemeinschaft DFG (grant no. Ha2611/1-1).

References

Bereiter-Hahn J, Vöth M (1988) Ionic control of locomotion and shape of epithelial cells: II. Role of monovalent cations. Cell Motility Cytoskeleton 10: 528–536

Binnig G, Quate CF, Gerber C (1986) Atomic force microscope. Phys Rev Lett 56: 930–933

Braet F, De Zanger R, Kämmer S, Wisse E (1997a) Noncontact versus contact imaging: an atomic force microscopic study on hepatic endothelial cells *in vitro*. Int J Imaging Syst Technol 8: 162–167

Braet F, De Zanger R, Wisse E (1997b) Drying cells for SEM, AFM and TEM by hexamethyldisilazane – a study on hepatic endothelial cells. J Microsc 186: 84–87

Bustamante JO, Liepins A, Prendergast RA, Hanover JA, Oberleithner H (1995) Patch clamp and atomic force microscopy demonstrate TATA-binding protein (TBP) interactions with the nuclear pore complex. J Membr Biol 146: 263–272

Butt H-J, Prater CB, Hansma PK (1991) Imaging purple membranes dry and in water with the atomic force microscope. J Vac Sci Technol 9: 1193–1196

Chen W-T (1981) Mechanism of retraction of the trailing edge during fibroblast movement. J Cell Biol 90: 187–200

Drake B, Prater CB, Weisenhorn AL, Gould SAC, Albrecht TR, Quate CF, Channell DS, Hansma HG, Hansma PK (1989) Imaging crystals, polymers, and processes in water with the atomic force microscope. Science 243: 1586–1589

Erlandsson R, Olsson L (1994) The study of biomolecules on surfaces using the scanning force microscope. In: Bongrand P, Claesson PM, Curtis ASG (eds) Studying cell adhesion. Springer, Berlin Heidelberg New York, pp 51–63

Florin E-L, Moy VT, Gaub HE (1994) Adhesion forces between individual ligand-receptor pairs. Science 264: 415–417

Fritz M, Radmacher M, Gaub HE (1994) Granula motion and membrane spreading during activation of human platelets imaged by atomic force microscopy. Biophys J 66: 1328–1334

Fuhr G, Richter E, Zimmermann H, Hitzler H, Niehus H, Hagedorn R (1998) Cell traces – footprints of individual cells during locomotion and adhesion. Biol Chem 379: 1161–1173

Hansma PK, Cleveland JP, Radmacher M, Walters DA, Hillner PE, Bezanilla M, Fritz M, Vie D, Hansma HG, Prater CB, Massie J, Fukunaga L, Gurley J, Elings V (1994) Tapping mode atomic-force microscopy in liquids. Appl Phys Lett 64: 1738–1740

Hasse C, Klöck G, Schlosser A, Zimmermann U, Rothmund M (1997) Parathyroid allotransplantation without immunosuppression. Lancet 350: 1296

Hay ED (1985) Interaction of migrating embryonic cells with extracellular matrix. Exp Biol Med 10: 174–193

Henderson E (1994) Imaging of living cells by atomic force microscopy. Prog Surf Sci 46: 39–60

Hofmann UG, Rotsch C, Parak WJ, Radmacher M (1997) Investigating the cytoskeleton of chicken cardiocytes with the atomic force microscope. J Struct Biol 119: 84–91

Hoh JH, Schoenenberger C-A (1994) Surface morphology and mechanical properties of MDCK monolayers by atomic force microscopy. J Cell Sci 107: 1105–1114

Hörber JKH, Mosbacher J, Häberle W, Ruppersberg JP, Sakmann B (1995) A look at membrane patches with a scanning force microscope. Biophys J 68: 1687–1693

Hornung J, Müller T, Fuhr G (1996) Cryopreservation of anchorage-dependent mammalian cells fixed to structured glass and silicon substrates. Cryobiol 33: 260–270

Ikai A (1996) STM and AFM of bio/organic molecules and structures. Surf Sci Rep 26: 261–332

Krüger D, Anczykowski B, Fuchs H (1997) Physical properties of dynamic force microscopies in contact and noncontact operation. Ann Phys 6: 341–363

Mullins RD, Stafford WF, Pollard TD (1997) Structure, subunit topology, and actin-binding activity of the arp2/3 complex from *Acanthamoeba*. J Cell Biol 136: 331–343

Mullins RD, Heuser JA, Pollard TD (1998) The interaction of arp2/3 complex with actin: nucleation, high affinity pointed end capping, and formation of branching networks of filaments. Proc Natl Acad Sci USA 95: 6181–6186

Oberleithner H, Schneider SW, Henderson RM (1997) Structural activity of a cloned potassium channel (ROMK1) monitored with the atomic force microscope: the ''molecular-sandwich'' technique. Proc Natl Acad Sci USA 94: 14144–14149

Palecek SP, Schmidt CE, Lauffenburger DA, Horwitz AF (1996) Integrin dynamics on the tail region of migrating fibroblasts. J Cell Sci 109: 941–952

Radmacher M, Tillmann RW, Fritz M, Gaub HE (1992) From molecules to cells: imaging soft samples with the atomic force microscope. Science 257: 1900–1905

Richter E, Fuhr G, Müller T, Shirley S, Rogaschewski S, Reimer K, Dell C (1996) Growth of anchorage-dependent mammalian cells on microstructures and microperforated silicon membranes. J Mater Sci Mater Med 7: 85–97

Sackmann E (1994) Intracellular and extracellular macromolecular networks – physics and biological function. Macromol Chem Phys 195: 7–28

Small JV, Anderson K, Rottner K (1996) Actin and the coordination of protrusion, attachment and retraction in cell crawling. Biosci Rep 16: 351–368

Welch MD, DePace AH, Verma S, Iwamatsu A, Mitchison TJ (1997) The human arp2/3 complex is composed of evolutionarily conserved subunits and is localized to cellular regions of dynamic actin filament assembly. J Cell Biol 138: 375–384

Yamagata M, Saga S, Kato M, Bernfield M, Kimata K (1993) Selective distributions of proteoglycans and their ligands in pericellular matrix of cultured fibroblasts. J Cell Sci 106: 55–65

Zimmermann U, Klöck G, Federlin K, Hannig K, Kowalski M, Bretzel RG, Horcher A, Entenmann H, Sieber U, Zekorn T (1992) Production of mitogen-contamination free alginates with variable ratios of mannuronic acid to guluronic acid by free flow electrophoresis. Electrophoresis 13: 269–274